Heliyon 8 (2022) e11495

Contents lists available at ScienceDirect

Heliyon

journal homepage: www.cell.com/heliyon

Research article

Adipose-derived stem cell-secreted exosomes enhance angiogenesis by promoting macrophage M2 polarization in type 2 diabetic mice with limb ischemia via the JAK/STAT6 pathway

Xiangkui Wang [a,b,1], Shiyuan Chen [c,1], Ran Lu [c], Yong Sun [c], Tao Song [c], Zhonglin Nie [c], Chaowen Yu [c], Yong Gao [a,c,*]

[a] Jinan University, 601 Huangpu Avenue West, Tianhe District, Guangzhou, 510632, Guangdong, China
[b] Department of Vascular Surgery, Huaibei General Miner Hospital, No. 1 Changshan North Road, Xiangshan District, Huaibei, 235000, Anhui, China
[c] Department of Vascular Surgery, The First Affiliated Hospital of Bengbu Medical College, 287 Changhuai Road, Bengbu, 233004, Anhui, China

ARTICLE INFO

Keywords:
Adipose-derived stem cells (ADSCs)
Exosomes
Macrophages
Polarization
Diabetic limb ischemia

ABSTRACT

Diabetic lower limb ischemia is an intractable disease that leads to amputation and even death. Recently, adipose-derived stem cell-secreted exosomes (ADSC-Exo) have been reported as a potential therapeutic approach, but its specific mechanism of action is unknown. Studies have found that exosomes derived from stem cells can reduce inflammation and promote tissue repair. Macrophages play an important role in the development and repair of inflammation in lower limb ischemic tissue, but the specific regulation of ADSC-Exo in macrophages has rarely been reported. The present study aimed to verify whether ADSC-Exo could promote angiogenesis by regulating macrophages to reduce the level of inflammation in diabetic ischemic lower limbs. In this study, adipose-derived stem cells (ADSCs) were obtained and identified, and ADSC-Exos were isolated using ultracentrifugation and characterized using transmission electron microscopy, nanoparticle tracking analysis, and western blotting analysis. The uptake of ADSC-Exos by macrophages was observed using immunofluorescence, and macrophage polarization induced by ADSC-Exos was identified by flow cytometry, immunofluorescence and ELISA. The effects of ADSC-Exos on the proliferation, apoptosis, migration and adhesion of macrophages were evaluated using CCK-8 assay, flow cytometry, Transwell assay, scratch and adhesion experiments, and ELISA assay. The polarization-related JAK/STAT6 signaling pathway was explored by using western blotting. A lower limb ischemic model of type 2 diabetic mice was established and ADSC-Exos was intramuscularly injected into the mice. The blood flow in the lower limbs was assessed using a laser Doppler flowmeter, while the level of angiogenesis was determined using immunohistochemistry and immunofluorescence. The results of this study prove that ADSC-Exos induced M2-phenotype polarization of macrophages via the JAK/STAT6 signaling pathway can promote the proliferation, migration and adhesion of M2 macrophages, inhibit the apoptosis of macrophages, and promote the angiogenesis and revascularization of ischemic lower limbs in type 2 diabetic mice. Thus, this study provides a theoretical and experimental basis for the clinical treatment of diabetic lower limb ischemic disease.

1. Introduction

The development of increasingly prosperous societies has resulted in an increase in the morbidity rate of diabetic lower limb ischemic disease, which often leads to amputation or even death. At present, the clinical treatment of diabetic lower limb ischemic disease mainly uses drugs and surgical revascularization, which produce an unsatisfactory level of long-term efficacy [1].

Mesenchymal stem cells (MSCs) are self-renewing cell with multi-directional differentiation potential, and are ideal seed cells for regenerative medicine and tissue engineering [2, 3]. Adipose-derived stem cells (ADSCs) are MSCs with the advantages of being easy to obtain, abundant, and of high purity. ADSCs have a strong multi-directional differentiation potential, high time-dependent differentiation ability, and rapid rate of proliferation, and are thus considered as ideal for the treatment of ischemic diseases [4]. Emerging evidence has shown that MSCs mainly

* Corresponding author.
E-mail addresses: gaoyongbbyxy@163.com, 0000731@bbmc.edu.cn (Y. Gao).
[1] Xiangkui Wang and Shiyuan Chen contributed equally to this work.

https://doi.org/10.1016/j.heliyon.2022.e11495
Received 31 May 2022; Received in revised form 21 August 2022; Accepted 4 November 2022

function via paracrine signaling rather than differentiation, while exosomes are important in intercellular communication and have been confirmed as important paracrine factors that can regulate MSCs [5].

Exosomes are membrane-bound vesicles wrapped in a lipid bilayers that are 30–100 nm in diameter, and are mainly involved in material exchange and signal transduction between cells [6]. Recent studies have demonstrated the homogeneous functions of MSC-derived exosomes in MSC tissue repairing and regeneration, inhibition of inflammation and the regulation of immune responses [7, 8]. Moreover, MSC-derived exosomes have the advantages of being safe from immune rejection and are stable in nature, the ability of passing through the blood-brain barrier and the placental barrier, the ability to target specific organs and damaged parts by exerting a direct effect, controllable production cost with convenience in transportation and storage, and the ability of being genetically modified for certain therapeutic purposes. Due to their favorable biological properties and advantages in therapeutic application, MSC-derived exosomes have become a research focus for tissue repair [9, 10, 11].

As important effector cells of the innate immunity, macrophages play a crucial role in the initiation, development, and resolution of inflammation. Macrophages can be activated through different pathways and functional states. After pathogens invade the human body, macrophages are polarized into the M1 phenotype, which play a pro-inflammatory role and can produce IL-1β, IL-6, TNF-α, and iNOS, which are inflammatory factors. The M1 phenotype is able to kill microorganisms, remove debris, and promote inflammatory responses, while the inflammatory factors produced induce macrophage apoptosis. M2 macrophages play an anti-inflammatory role and secrete VEGF, IL-10, and TGF-β, which can eliminate inflammation and promote wound healing, tissue repair, and regeneration and angiogenesis [12, 13]. Studies have found that MSC-derived exosomes can induce macrophage polarization into the M2 phenotype, improve cardiac injury following myocardial infarction, delay the formation of atherosclerotic plaques, and accelerate wound healing [14, 15, 16].

Diabetic patients are in a state of persistent hyperglycemia, which leads to the accumulation of advanced glycation end products, tissue inflammation and oxidative stress, resulting in impaired endothelial cell functions and angiogenesis [17, 18]. Angiogenesis is a key mechanism for vascular repair of ischemic tissues of the lower limbs. Thus, we suggest that ADSC-derived exosomes (ADSC-Exos) induce macrophage polarization into the M2 phenotype to eliminate inflammation, which promotes the angiogenesis of diabetic limb ischemia. Therefore, in the present study, we obtained and isolated ADSC-Exos, verified the induction ability of ADSC-Exos on macrophage polarization through the JAK/STAT6 signaling pathway, as well as the effects of ADSC-Exos on the proliferation, apoptosis, migration, and adhesion of M2 macrophages, and tested the effects of ADSC-Exos on angiogenesis in the hindlimb ischemia of mice with type 2 diabetes, which provided insights into potential therapeutic methods for diabetic lower extremity ischemic diseases in a clinical setting.

2. Methods

2.1. Animals

Wild-type (WT) C57/BL female mice that were 6 weeks old and type 2 diabetes mellitus (T2DM) C57BL/KsJ-db/db (db/db) mice that were 12 weeks old were purchased from SLAC Laboratory Animal Co., Ltd. (Shanghai, China) and housed under specific pathogen-free (SPF) conditions. The animal experiments conducted in this study were approved by the Ethics Committee of the First Affiliated Hospital of Bengbu Medical College and were performed in accordance with the “Guide for Care and Use of Laboratory animals” of Bengbu Medical College.

2.2. Isolation, culture, and identification of the ADSCs

Six-week-old female WT C57/BL6 mice were sacrificed after adequate anesthesia was administered, and adipose tissue under the groin and armpits were obtained through aseptic operation. Then, the adipose tissues were fully digested using NB4 collagenase (SERVA, Germany), and shaken in a shaker for 2 h. The homogenate and tissue fragments were seeded onto a Petri dish, and glucose (1 g/L), 10% fetal bovine serum (FBS), 100 U/mL penicillin, and 100 mg/mL streptavidin supplemented Dulbecco's Modified Eagle's Medium (DMEM) was added at 37 °C and in a 5% CO_2 atmosphere. The third-to fifth-generation of the ADSCs were obtained, washed with phosphate buffered saline (PBS) 3 times, and anti-mouse antibodies against CD34, CD45, CD90, CD105, and CD106 were co-incubated with ADSCs in the dark at 4 °C for 25 min. Isotype antibodies were used as the negative controls. Then, the cells were washed using PBS three times and analyzed using flow cytometry. For the identification of the ADSCs' ability of multiple differentiation, after the induction of ADSCs, the oil red staining was performed to identify the adipogenic differentiation and the alizarin red staining was performed to identify the osteogenic differentiation.

2.3. Isolation and identification of the ADSC-Exos

ADSC-derived exosomes (ADSC-Exos) were isolated, as previously reported [19]. In brief, the ADSCs and the culture medium were centrifuged at 300 × g for 10 min, and the supernatant collected was centrifuged at 2,000 × g for 10 min, and again collected the supernatant and centrifuged it at 10,000 × g for 3 h. Finally, the pellet collected was dissolved in PBS. Then, the exosomes obtained were subjected to Nanoparticle Tracking Analysis (NTA) (Zeta View PMX 110, Particle Metrix, Meerbusch, Germany) to measure their diameter. Briefly, the sample pool was rinsed with deionized water, and the Zeta View PMX110 was calibrated with polystyrene microspheres (110 nm), then the sample cells were diluted with 1 ×PBS buffer and subjected for detection. And the exosomes were observed and photographed under a transmission electron microscope (TEM) for morphological identification. The expression levels of CD63, HSP70, and TSG101, which are markers of exosomes, were identified using western blotting, while β-actin was applied as the internal control.

2.4. Exosome uptake by macrophages and the polarization of macrophages treated with ADSC-Exos

The mouse macrophage cell line, RAW264.7, was purchased from the Cell Bank of Type Culture Collection of The Chinese Academy of Sciences (Shanghai, China). Then, at a concentration of 100 μg/mL the RAW264.7 macrophages were co-cultured with ADSC-Exos labeled with CM-Dil (Abcam, UK) dye in high-glucose (4.5 g/L) DMEM supplemented with 10% FBS and 1% antibiotic/antimycotic solution (Gibco, USA) at 37 °C in a 5% CO_2 atmosphere for 24 h. The nuclei of the macrophages were stained with 2-(4-Amidinophenyl)-6-indolecarbamidine dihydrochloride (DAPI). Immunofluorescence microscopy was applied to confirm phagocytosis of the ADSC-Exos by the macrophages and images of this process were captured.

The RAW264.7 macrophages and 100 μg/mL of ADSC-Exos were co-cultured under high glucose for 48 h at 37 °C in a 5% CO_2 atmosphere. RAW264.7 macrophages without ADSC-Exos were used as the control. The nuclei of the macrophages were stained with DAPI, while the macrophages were stained with antibodies of the M2 phenotype macrophage-specific markers, CD206 (Abeam, UK), CD163 (Abeam, UK), and the M1 macrophage-specific marker, iNOS (Abeam, UK), respectively. The cells were observed and photographed under an immunofluorescence microscope, and fluorescence intensities were analyzed and compared using ImageJ software. The expression levels of CD206, CD163, and iNOS were determined using flow cytometry to confirm the polarization of the macrophages.

2.5. Proliferation and apoptosis assays of the macrophages

The effect of the ADSC-Exos on the proliferation of the RAW264.7 macrophages was explored using Cell Counting Kit 8 assay (CCK-8;

Abcam, UK). In brief, 2×10^3 cells/well of RAW264.7 macrophages were cultured in a 96-well plate under high glucose along with either an equal volume of DMEM, 25 μg/mL ADSC-Exos, 50 μg/mL ADSC -Exos, or 100 μg/mL ADSC-Exos at 37 °C in a 5% CO_2 atmosphere. Next, 10 μL of CCK-8 solution was added into each well at 0, 12, 24, and 48 h. The optical density (OD) at a wavelength of 450 nm was analyzed using a microplate spectrophotometer. At the same time, the optimal concentration of ADSC-Exos that should be used to promote the proliferation of RAW264.7 macrophages was confirmed for use in subsequent experiments.

The effect of ADSC-Exos on the apoptosis of RAW264.7 macrophages was detected using flow cytometry. RAW264.7 macrophages were co-incubated under low glucose (1 g/L), high glucose (4.5 g/L) conditions, or high glucose +100 μg/mL ADSC-Exos at 37 °C in a 5% CO_2 atmosphere for 48 h. The apoptosis rate of the RAW264.7 macrophages was measured using an Annexin V-FITC/PI Apoptosis Detection Kit (Yeasen Biotechnology Co., Ltd., Shanghai, China) and flow cytometry, as previously described [20]. Statistical comparison of the proportion of Annexin V^+/PI-early apoptotic cells was conducted.

2.6. Migration and adhesion assay of macrophages

Wound-healing assay and Transwell assay were performed to verify ADSC-Exos' effects on the migration of RAW264.7 macrophages under high glucose. For wound healing assay, 5×10^5 RAW264.7 macrophages were first inoculated into a 6-well plate, streaked 12 h later with a sterile 20 μL pipette tip, then washed 3 times with sterile PBS, added with 100 μg/mL ADSC-Exos and high-glucose DMEM, observed and photographed at 0 and 24 h using an inverted microscope. The area of wound healing was analyzed using Image J software.

For Transwell assay, 0.2 ml of RAW264.7 macrophages at 10^5 cells/ml were inoculated into Transwell chambers with Matrigel (Corning, USA), and 0.2 ml of high-glucose DMEM containing 100 μg/mL ADSC-Exos was added into the upper chamber. 0.7 ml DMEM was added into the lower chamber. After culturing under 37 °C for 24 h, 1 ml of 4% paraformaldehyde solution was added into per well and fixed for 15 min under 25 °C; then washed twice with PBS. 1 ml of 0.5% crystal violet solution was added into per well, washed three times with PBS after staining for 60 min, the cells in the upper chamber were wiped off with a cotton swab. An inverted microscope was applied to observe and take photographs. Cell numbers were analyzed using Image J software.

Adhesion experiments were performed to verify the effect of ADSC-Exos on the adhesion ability of RAW264.7 macrophages under high glucose environment. 100μL of coating solution was added to per well of the 96-well plate, and the culture plate was placed at 4 °C for 12 h, then the coating solution was removed, and the plate was dried and washed 3 times. RAW264.7 macrophages co-cultured with ADSC-Exos under high glucose condition for 24 h were seeded into 96-well plates at 5×10^4 cells/well. After incubation under 37 °C for 1 h, the medium was washed 3 times. Nuclei were stained with DAPI (Dako, Denmark) and observed under an immunofluorescence microscope and photographed to perform the cell number count. Each of the above experiments was performed in three wells and repeated three times.

2.7. Western blot assay of the signaling pathway in macrophages

Western Blot assay was conducted to explore polarization-related signaling pathways in macrophages after treated with 100 μg/mL ADSC-Exos for 24 h under high glucose. Western blot assay was performed as previously described [20]. Cell samples of the macrophages treated with or without ADSC-Exos and with ADSCs + GW4869 (Selleck, China) (an exosome inhibitor) were collected and total protein was extracted using RIPA lysate and centrifugation, and the protein concentration of the extracted total protein was confirmed following electrophoresis, transfer, blocking, and immunoreaction with the following antibodies: anti-JAK and P-JAK antibody, anti-STAT6 and P-STAT6 antibody, and anti-β-actin antibody (1:500; Abcam, UK). Then, the membrane was washed and chemiluminescence detection was performed to test the exposure of the film. Finally, data analysis of the gray value was performed using ImageJ software. For the verification of the inhibition effect of GW4869 on ADSC-Exos, the total protein content of exosomes extracted from the conditioned medium of both groups was measured using the BCA protein quantification kit. BSA was a protein standard and the operation was performed according to the kit instructions.

2.8. Establishment of a T2DM limb ischemic mouse model and treatment with ADSC-Exos

Twelve T2DM C57BL/KsJ-db/db male mice that were 12-weeks-old (SLAC Laboratory Animal Co., Ltd, China) were anesthetized using 3% isoflurane gas and anesthesia was maintained using 2% isoflurane. The right lower extremity of the mice was shaved, sterilized, and draped. A 8-mm incision was made from the groin until the inner thigh, and the femoral arteries were ligated distal to the common femoral artery and proximal to the superficial femoral artery using 8-0 sutures, under a 20× stereo microscope. The twelve mice were randomly divided into two groups, the ADSC-Exo group ($n = 6$) and the DMEM control group ($n = 6$). Then, 2 mL of DMEM or DMEM with 100 μg/mL of ADSC-Exos was injected into the gastrocnemius, gracilis, and quadricep muscles into the ADSC-Exo group ($n = 6$) and the DMEM control group of mice in the ADSC-Exo group and the DMEM control group, respectively, on day 1, 2, and 3. On the 1st, 7th, and 28th day after ADSC-Exo transplantation, the blood flow in both the lower extremities of the two groups of mice was detected using a laser Doppler perfusion imager.

2.9. Histological assay

The T2DM mice in both groups were sacrificed after gas anesthesia was induced on the 28th day to perform perfusion fixation. The muscles of both hindlimbs were completely excised and frozen sections were created as previously described [20]. After fixing, the samples were blocked and immunohistochemically stained using an antibody against CD31 (Abcam, UK), and were observed and photographed under a microscope. For the immunofluorescence staining of muscle slices, the microvessels were stained with FITC fluorescent anti-CD31 antibody (Abcam, UK) and the nuclei were stained with DAPI (Dako, Denmark), then observed and photographed under a fluorescence microscope.

2.10. Statistical analysis

All data are presented as mean ± standard deviation (SD). SPSS version 21.0 software (IBM Corp., USA) and GraphPad Prism version 9.0 (GraphPad, USA) were applied to analyze all statistics. Unpaired student t-test and two-way analysis of variance (ANOVA) were applied for the comparison of data between different groups. $P < 0.05$ was considered to indicate statistical significance.

3. Results

3.1. Isolation and identification of the ADSCs

The primary generation of the ADSCs were successfully extracted from the inguinal and axillary fat tissue of 6-week-old WT C57/BL6 mice. ADSCs of generations P3–P5 exhibited a typical spindle shape and a fibroblast-like shape (Figure 1A). Flow cytometry analysis demonstrated that the ADSCs were negative for CD34 and CD45 expression, while the expression of the mesenchymal stem cell markers, CD90, CD105, and CD106 were all strongly positive (Figure 1B, C, D, E, F). After 3 weeks of induction of adipocytes, oil red staining showed a large number of red-stained lipid droplets of different sizes in the cells (Figure S1A). After 3 weeks of ADSC induction into osteocytes, alizarin red staining

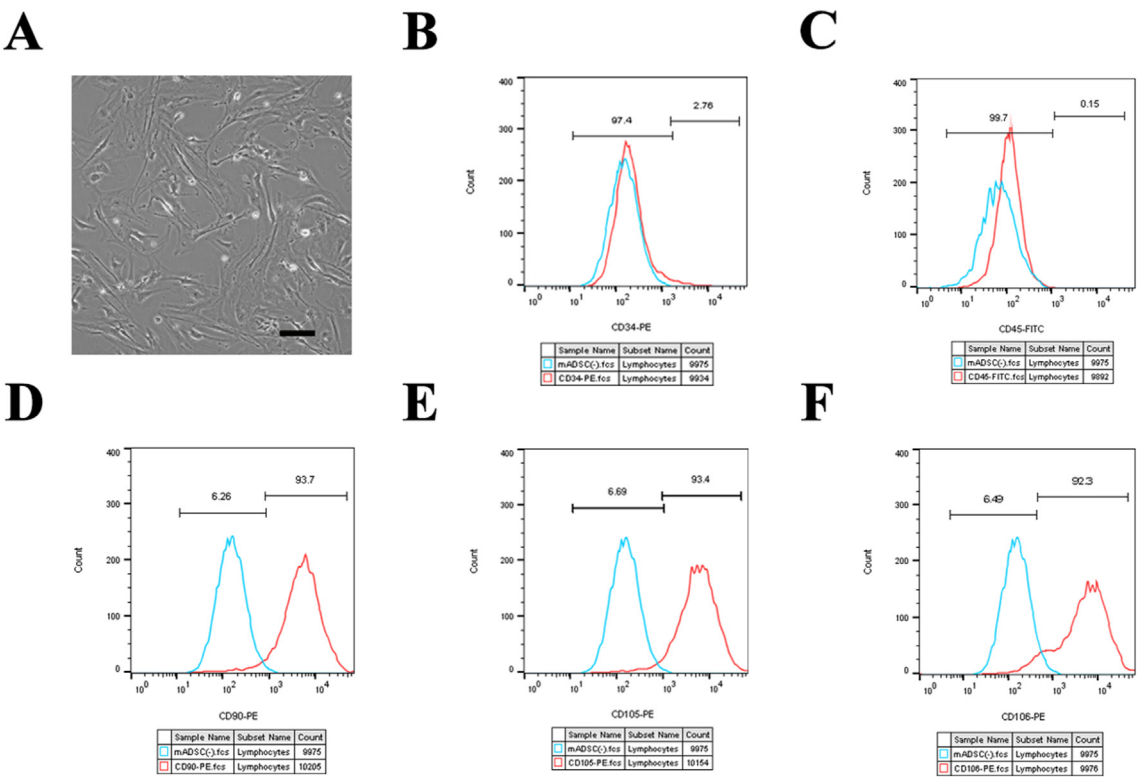

Figure 1. Characterization and identification of ADSCs. ADSCs of the P3–P5 generation exhibited a typical spindle shape and fibroblast-like shape (A). Flow cytometry demonstrated that the ADSCs were negative for CD34 (B) and CD45 (C) expression, while being strongly positive for the expression of mesenchymal stem cell markers, CD90 (D), CD105 (E), and CD106 (F). Scale bar = 100 μm P3, passage 3; P5, passage 5; ADSCs, Adipose-derived stem cells.

demonstrated a large number of scattered red calcium nodules were observed under the microscope (Figure S1B). The above results confirmed the high level of purity of the ADSCs obtained and were used in consequent experiments.

3.2. Isolation and identification of the ADSC-Exos

ADSC-Exos were successfully acquired and isolated, and were found to exhibit a typical "saucer-like" structure when observed under a TEM (Figure 2A). NTA analysis indicated that 97.8% of the ADSC-Exos had a diameter of 154.0 nm (Figure 2B). Western blotting and statistical analysis showed the expression of exosomal surface markers, such as CD63, HSP70, and TSG101 in ADSC-Exos (Figure 2C, 2D). The above results confirmed the high-purity of the ADSC-Exos obtained for use in consequent experiments.

3.3. Exosome uptake by macrophages and the effect of the ADSC-Exos on the polarization of the macrophages

High glucose conditions were applied to vastly mimic the hyperglycemia of clinical patients with diabetic lower limb ischemia. After co-incubating the RAW264.7 macrophages with 100 μg/mL ADSC-Exos under high glucose conditions for 24 h, they were observed under a fluorescence microscope. Red CM-Dil-labeled ADSC-Exos surrounded each blue DAPI-stained macrophage nucleus, demonstrating that ADSC-Exos were successfully phagocytosed by the macrophages (Figure 3A).

The effect of ADSC-Exos on macrophage polarization was verified using immunofluorescence staining. After co-incubating the RAW264.7 macrophages with 100 μg/mL ADSC-Exos under high glucose for 24 h, immunofluorescence staining was performed on the macrophages to determine the expression of the M2 phenotype markers, CD206 and CD163, and M1 phenotype marker iNOS. The results showed that the fluorescence intensity was significantly higher for iNOS ($P < 0.05$) (Figure 3B, 3D). At the same time, the flow cytometry assay demonstrated that the expression of CD206 and CD163 in macrophages treated with ADSC-Exos were significantly higher than that of macrophages without ADSC-Exos (M0) treatment under high glucose conditions. However, the change in the expression of iNOS was not significant (Figure 3C). The above results demonstrate that ADSC-Exos could induce the polarization of macrophages into to the M2 phenotype under high glucose conditions.

3.4. Effects of ADSC-Exos on the proliferation and apoptosis of macrophages

CCK-8 assay was applied to examine the effect of different concentrations of ADSC-Exos on the proliferation of macrophages. The results of the CCK-8 assay demonstrated that at 48 h, 100 μg/mL ADSC-Exos exerted a significantly higher promotion effect on macrophage proliferation ($P < 0.05$), compared with ≤100 μg/mL ADSC-Exos. Therefore, the optimum therapeutic concentration of ADSC-Exos on macrophages was 100 μg/mL under high glucose conditions (Figure 3E). Therefore, a therapeutic ADSC-Exos concentration of 100 μg/mL was selected to be used in subsequent *in vitro* and *in vivo* experiments.

The effect of ADSC-Exos on macrophage apoptosis was analyzed using flow cytometry. The apoptosis rate was calculated in early apoptotic cells using Annexin V+/PI−. The results of flow cytometry analysis demonstrated that the apoptosis rate of macrophages under high glucose conditions (8.7 ± 2.2%) was slightly higher, compared with low glucose conditions (8.4 ± 3.2%), but there was no statistical difference ($P > 0.05$), while the percentage of the apoptosis of macrophages co-cultured with ADSC-Exos under high glucose conditions (1.3 ± 0.7%) was significantly lower than the other two groups ($P < 0.01$) (Figure 3F, 3G). These results demonstrate that ADSC-Exos increased the rate of

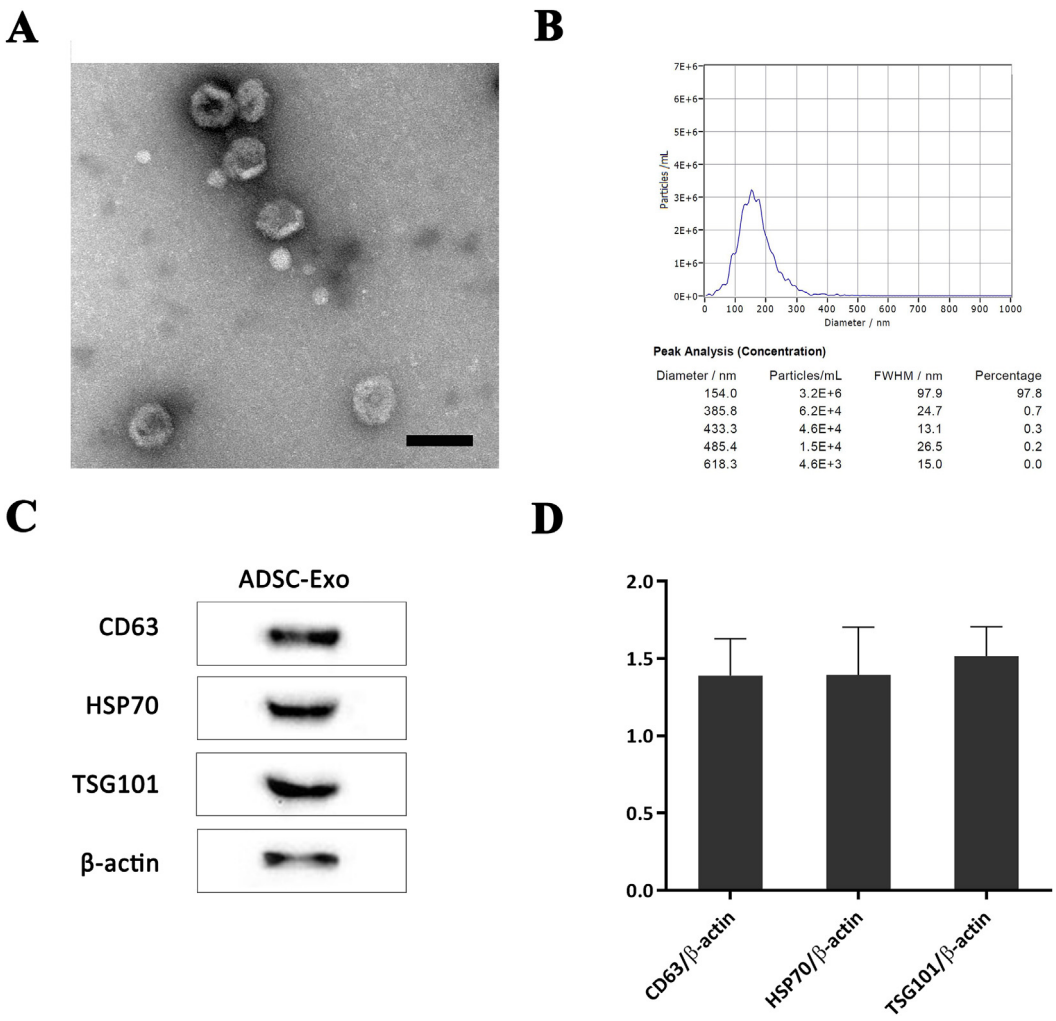

Figure 2. Characterization and identification of the ADSC-Exos. The exosomes exhibited a typical "saucer-like" shape when viewed under a TEM (A). NTA analysis indicated that 97.8% of the ADSC-Exos had a diameter of 154.0 nm (B). Western blotting (C) and statistical analysis (D) demonstrated the expression of exosomal surface markers of CD63, HSP70, and TSG101, in the ADSC-Exos. Scale bar = 100 μm. ADSC-Exos, Adipose-derived stem cell-derived exosomes.

proliferation and significantly inhibited the apoptosis of macrophages under high glucose conditions.

3.5. Effects of ADSC-Exos on the migration and adhesion of macrophages

Macrophages migrate and adhere onto damaged tissues and blood vessels *in vivo*. Therefore, the effects of ADSC-Exos on the migration and adhesion of macrophages were examined. The wound healing assay showed that macrophages incubated with ADSC-Exos under high glucose conditions migrated significantly faster than the control group (relative gap area, $P < 0.05$) (Figure 4A, 4B), within 24 h. The results of the Transwell assay showed that macrophages co-incubated with ADSC-Exos under high glucose conditions showed a significant increased in numbers compared with the control group ($P < 0.05$) (Figure 4C, 4D). Overall, these results confirm the promotional effect exerted by ADSC-Exos on macrophage migration.

For the adhesion assay, the adhered macrophages were stained with DAPI to visualize their nuclei. Statistical analysis showed that the number of macrophages that had adhered after co-incubated with ADSC-Exos under high glucose conditions was significantly higher than the control group ($P < 0.01$) (Figure 4E, 4F). Together these experimental results indicated that ADSC-Exos promoted the adhesion of macrophages under high glucose conditions.

3.6. Effects of ADSC-Exos on the polarization-related signaling pathway in macrophages

The previous experiments showed that ADSC-Exos induced the polarization of macrophages into a M2 phenotype. Previous studies have shown that STAT6 plays an important role in the regulation of M2 phenotype macrophage-specific target genes, such as Arg-1. STAT6 is the most important molecule in the IL-4-mediated signaling pathway, while the JAK/STAT6 pathway is the most important pathway involved in signal transduction from the cell membrane to the nucleus [21]. Therefore, in this study we explored the JAK/STAT6 signaling pathway. Western blotting demonstrated that the phosphorylation levels of JAK and STAT6 were significantly elevated in macrophages treated with ADSC-Exos, compared with macrophages treated with DMEM, under high glucose conditions ($P < 0.05$). Then, the exosome inhibitor, GW4869, was added into the ADSC medium and the supernatant was collected and ultracentrifuged, and the macrophages were treated with the centrifuged components. However, the phosphorylation levels of JAK and STAT6 were only slightly elevated without a statistical difference ($P > 0.05$) (Figure 5A, 5B). These results confirmed that ADSC-Exos activates the JAK/STAT6 signaling pathway, which is important for macrophage polarization into the M2 phenotype. For the verification of the inhibition effect of GW4869 on ADSC-Exos, the BCA method was used to

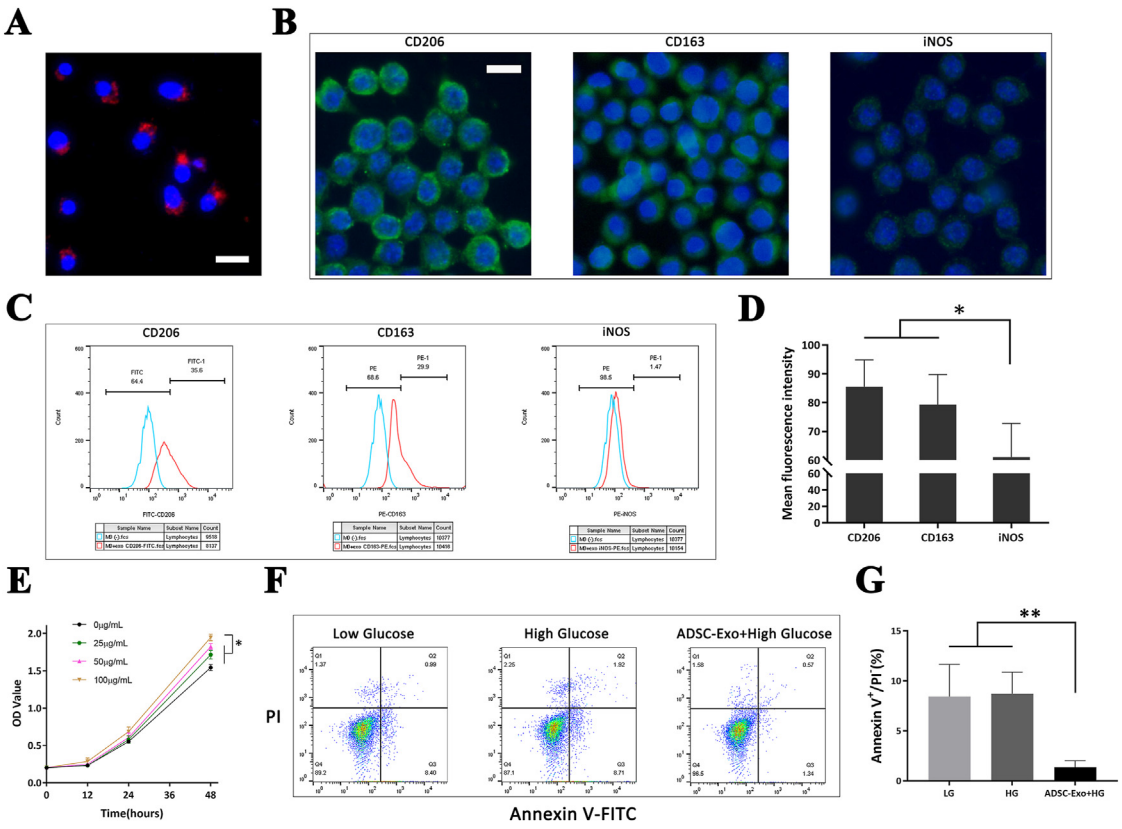

Figure 3. Exosome uptake by macrophages and the effects of ADSC-Exos on the polarization, proliferation, and apoptosis of macrophages. Red CM-Dil-labeled ADSC-Exos surrounded each blue DAPI-stained macrophage nucleus (A). CD206 and CD163 fluorescence intensity were significantly higher than that of iNOS in the ADSC-Exos-treated macrophages (B, D). Flow cytometry showed a higher expression of CD206 and CD163 but similar iNOS in the ADSC-Exos-treated macrophages under high glucose conditions (C). The CCK-8 results demonstrated that at 48 h, 100 μg/mL ADSC-Exos exerted a significantly higher promotion effect on macrophage proliferation (E). Flow cytometry demonstrated that the apoptosis of macrophages co-cultured with ADSC-Exos under high glucose conditions was significantly lower than that of the other two groups (F, G). Scale bar = 20 μm; *, $P < 0.05$; **, $P < 0.01$. ADSC-Exos, Adipose-derived stem cell-derived exosomes.

measure the protein levels of exosomes extracted from ADSC-Exos and ADSC-Exos + GW4869 conditioned medium. The exosomal protein level of the GW4869 treated group was significantly lower than that of the ADSC-Exos control group ($P < 0.05$) (Figure S2).

3.7. Effects of ADSC-Exos on angiogenesis and blood perfusion in the T2DM limb ischemic mice

A simple low-ligation model of femoral artery in T2DM mice was successfully constructed. The advantage of this model is the low occurrence of acute limb ischemic necrosis, which is similar to the pathophysiological process of clinical diabetic chronic ischemia. Laser Doppler perfusion imager scans were performed on mice on the first day, first week, and fourth week to assess blood perfusion in the hindlimbs (Figure 5E). Statistical analysis showed that blood perfusion in mice of both groups was similar on the first day after the transplantation of ADSC-Exos or DMEM, but the difference between the two groups began to be obvious on the seventh day. On the 28th day, the blood perfusion ratio of the ADSC-Exos group was significantly higher than that of the DMEM control group ($P < 0.05$) (Figure 5F).

Immunohistochemical staining of CD31 in the muscles of the lower extremities of T2DM mice demonstrated that microvessel density in the ADSC-Exo group was significantly higher than that of the DMEM control group ($P < 0.05$) (Figure 5C, 5D). Immunofluorescence staining of CD31 and DAPI nuclei also demonstrated that microvessel density in the ADSC-Exo group was significantly higher than that of the DMEM control group ($P < 0.05$) (Figure 5G, 5H). The results of the *in vivo* experiments demonstrated that ADSC-Exos promotes angiogenesis and blood perfusion in the T2DM mouse limb chronic ischemia model.

4. Discussion

In this study, ADSC-Exos were steadily obtained and the positive effect of ADSC-Exos on the M2-phenotype polarization of macrophages, the enhancement of ADSC-Exos on the viability, migration and adhesion of macrophages under high glucose condition *in vitro*, and the promotion of ADSC-Exos on angiogenesis and revascularization in the ischemic lower extremities of the T2DM mice *in vivo* were verified. Furthermore, the activation of the JAK/STAT6 pathway may be the mechanism by which M2 polarization is induced by ADSC-Exos under high glucose conditions.

Stem cell exosome transplantation has become a hot topic in the field of tissue engineering during recent years. As an important participant in intercellular communication, stem cell-derived exosomes not only contain the genetic information of stem cells (proteins, mRNAs, microRNAs, etc.), but also can transfer certain molecules into target cells, inheriting many advantages of stem cell therapy. Stem cell-derived exosomes may be superior to ordinary cell-derived exosomes in terms of their therapeutic effect and diversification of treatment pathways, and are superior to pure stem cell therapy in terms of application range, precise dose control, and avoidance of immunological rejection. Stem cell-derived exosomes are more widely regulated and can repair or prevent damages caused by diabetic complications through multiple mechanisms [22]. As a novel cell-free therapy, stem cell-derived exosomes occupy a unique position and broad prospects for clinical applications. Several studies have demonstrated that stem cell-derived exosomes play a pivotal role in the inflammatory, angiogenesis, re-epithelialization and remodeling stages of diabetic lower extremity ischemic disease [23]. Exosomes are usually endocytosed by target cells or fused with the cell membrane to release internal miRNAs, proteins and other bio-functional

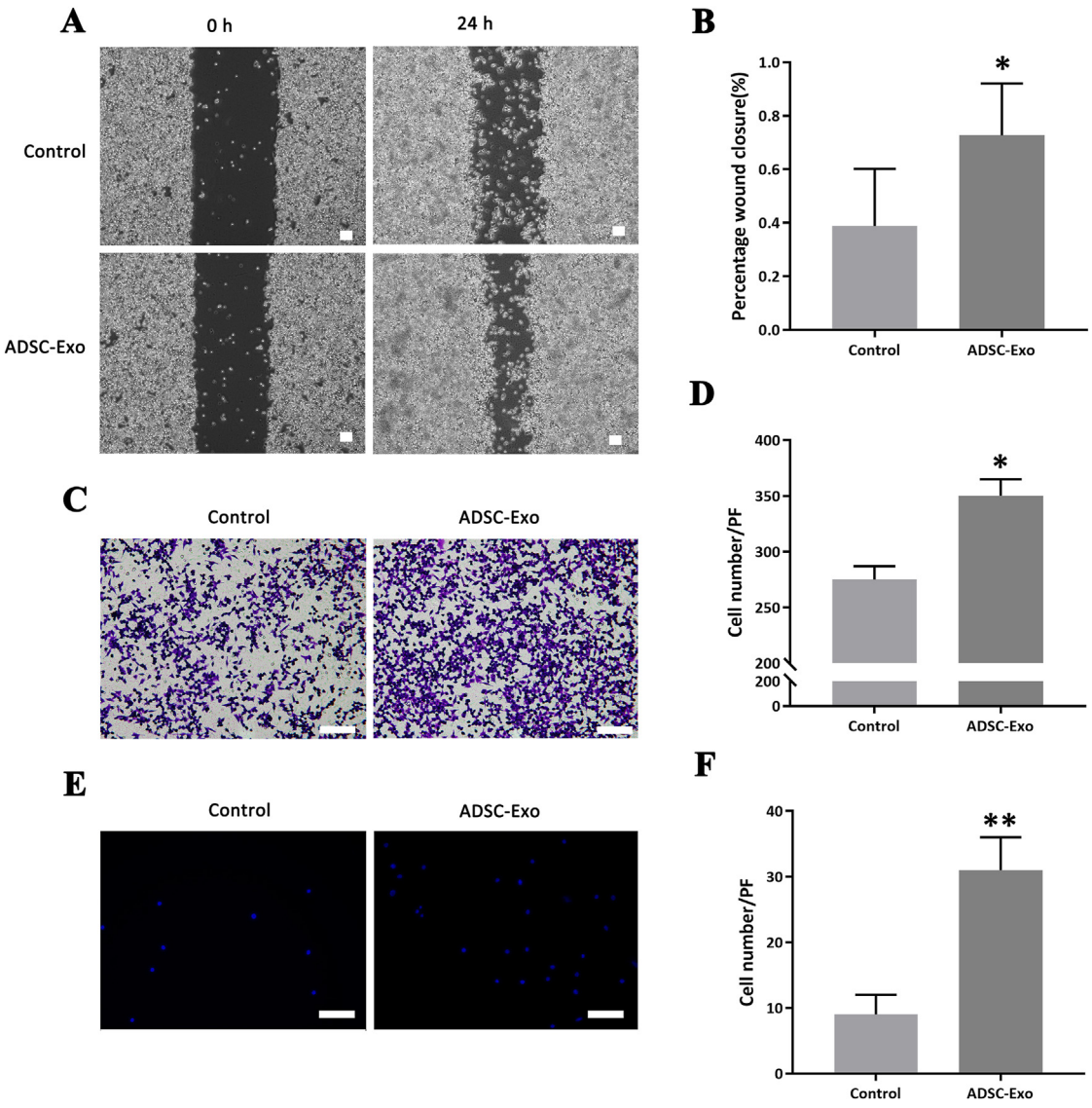

Figure 4. Wound healing, Transwell, and adhesion assays of the macrophages. The results of the wound healing assay showed that macrophages incubated with ADSC-Exos under high glucose conditions migrated significantly faster than the control group (A, B). The Transwell assay showed that macrophages co-incubated with ADSC-Exos under high glucose conditions showed a significant increase in number (C, D). The adhesion assays showed that the number of macrophages that adhered in the group co-incubated with ADSC-Exos under high glucose conditions was significantly higher (E, F). Scale bar = 100 μm; *, $P < 0.05$; **, $P < 0.01$. ADSC-Exos, Adipose-derived stem cell-derived exosomes.

factors. The miRNAs often bind to target mRNAs in the cytoplasm and affect the translation process. Proteins also function primarily in the cytoplasm. Therefore, it has less effect on the transcription process in the nucleus. MSC-derived exosomes may contain miRNAs and proteins, such as nuclear factor erythroid-related factor 2 (NRF2), miR-21, miR-23a, miR-124a, miR126, lncRNAH19, let-7b, and miR132. MSC-derived exosomes activate targeted signaling pathways to regulate immune response, autophagy, and angiogenesis, and plays an crucial role in promoting tissue and cell regeneration [24, 25], but the specific mechanism by which MSC-derived exosomes promote angiogenesis remain to be further studied.

The main cause and feature of diabetic lower extremity ischemic disease is chronic persistent hyperglycemia, which can lead to the chronic inflammation of blood vessels, which gradually destroys blood vessels, and subsequently to vascular occlusion and tissue ischemia [26]. Therefore, we focused our attention on macrophages, which are the most important effector cells in inflammation response. Studies have shown that ischemia can lead to the apoptosis and necrosis of tissues, and macrophages have been shown to play an important role in apoptosis and necrosis, tissue clearance, repair or reconstruction, and angiogenesis after ischemia [27]. Macrophages perform a key role in the vascular regeneration process and have great therapeutic potential. Macrophages differentiate into M1 phenotype pro-inflammatory cells and M2 phenotype anti-inflammatory cells under different environmental stimuli [28]. In the animal models of myocardial infarction and stroke, macrophages have been shown to be positively associated with angiogenesis [29, 30]. Macrophages play important roles in various microvascular regeneration processes, such as local ECM modification, induction of EC migration or proliferation. Macrophages induce angiogenesis by expressing MMPs and degrade the capillary endothelial extracellular matrix, thereby promoting endothelial cell migration. They can tunnel into the stroma, in which endothelial progenitor cells or capillary sprouts grow. M2 phenotype macrophages also exert anti-inflammatory effects, secrete IL-6, VEGF, IL-10, and TGF-β, and cause effective efferocytosis to clear apoptotic cells, which promotes wound healing, tissue repair and regeneration, and angiogenesis. Using mouse myocardial infarction and atherosclerosis models and rat diabetic ulcer models, it has been confirmed that mesenchymal stem cell exosomes can promote the polarization of

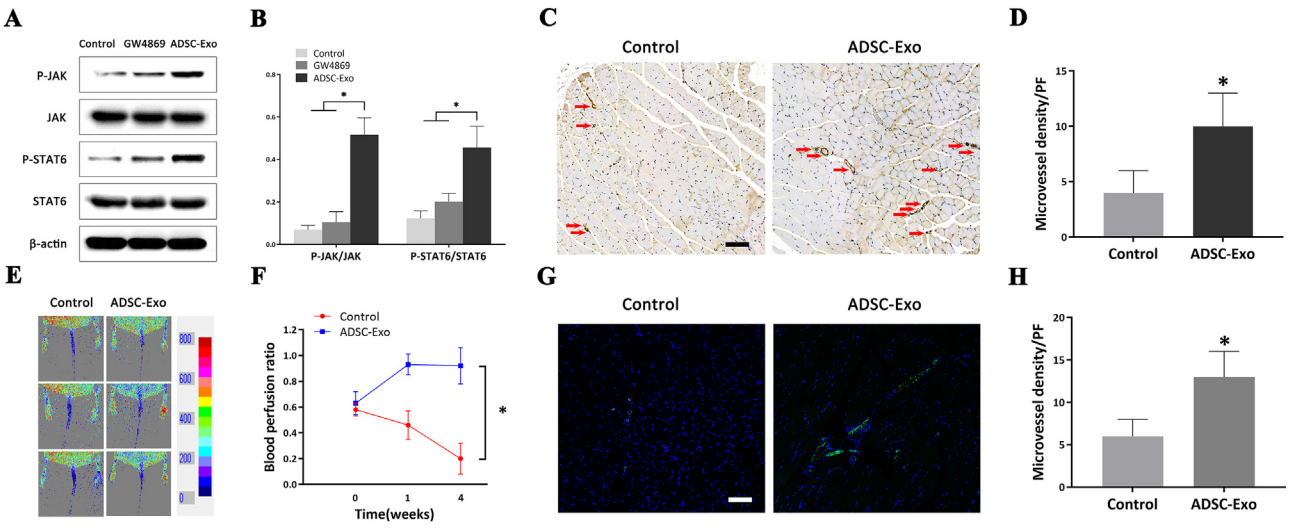

Figure 5. Signaling pathway of M2 macrophage polarization *in vitro*, blood perfusion and histological analysis of the T2DM mouse limb ischemia model *in vivo* after ADSC-Exo transplantation. Western blotting assay of the signaling pathway showed that the M2 polarization-associated JAK/STAT6 pathway had been activated (A, B). Blood flow in hindlimbs was examined using a laser Doppler perfusion imager on days 1, 7, and 28 (E). Statistical analysis showed a significantly higher blood perfusion rate in the ADSC-Exo group than in the DMEM control group (F). Immunohistochemistry staining of CD31 in the hindlimb muscles showed a significantly higher vascular density in the ADSC-Exo group (C, D). Immunofluorescence staining of CD31 (green) and DAPI (blue) demonstrated a significantly higher vascular density in the ADSC-Exo group (G, H). Scale bar = 100 μm; *, $P < 0.05$; ADSC-Exos, Adipose-derived stem cell-derived exosomes.

macrophages into the M2 type, but the underlying mechanisms have not been fully elucidated [14]. At the same time, as far as we know, there have been no reports published on the role and mechanism by which MSC-derived exosomes promote M2 macrophage polarization in diabetic lower extremity ischemic diseases, which has been the basis of research and innovation in this study.

In this study, we compared between the experimental group, the control group, and the group to which the exosome inhibitor, GW4869, and found that ADSC-Exo could significantly activate the JAK/STAT6 signaling pathway in macrophages, which may partly explain the mechanism by which ADSC-Exos induce the polarization of macrophages towards the M2 phenotype. It is well known that the JAK-STAT pathway is the canonical pathway that leads to the M2 polarization of macrophages. JAK1 is a member of the Janus kinase family and is associated with components of the IL-4R complex [31]. After IL-4/IL-13 binds to receptors located in the cell membrane, JAK1 is instantly phosphorylated, activating STAT6, which leads to the activation of M2-like genes, such as YM1, Arg1, Fizz1, IL-10, and MGL1 [32,33], resulting in the polarization of macrophages towards the M2 phenotype. It is worth noting that there are other pathways, such as the Akt-p18-mTOR-LXR pathway and the ABCA1-PKA pathway, which lead to the M2 phenotype polarization of macrophages. Therefore, it remains to be determined whether ADSC-Exos also promotes the M2 polarization of macrophages through these pathways and requires further validation through future experiments.

There are two other points that are worth noting in this study. The first is that we used a simple low ligation model of the femoral artery in the T2DM mice, which could simulate the clinical symptoms of peripheral arterial disease in patients with T2DM, since in clinical practice diabetic lower extremity ischemia is a chronic process, in which acute lower extremity ischemia rarely occurs. Whereas the commonly used femoral artery ligation model often results in acute critical lower extremity ischemia in mice and limb necrosis on about the seventh day. The lower limbs suffer from complete necrosis and severe tissue loss, which is beyond the scope of cell transplanting therapy, which make it difficult to accurately evaluate the actual therapeutic effect of cell and exosome transplantation. In contrast, the pathophysiological processes in the simple low ligation model of the femoral artery mainly include vascular bed remodeling, chronic capillary loss, neovascularization damage, and ischemia deterioration [34, 35]. Therefore, blood perfusion in the affected limb can be better assessed to determine methods that can be used to preserve limb integrity. In our model, even on day 28, the limbs were still affected in all three groups, but the level of blood perfusion was completely different. Another interesting point is that blood perfusion in the experimental group was slightly lower on the 28th day than that of the seventh day. This difference may be due to the limited time for which exosomes exist *in vivo*. Therefore, the mechanism by which we can achieve the slow release of exosomes in damaged tissues to induce a long-lasting therapeutic role as a future direction for subsequent research.

4.1. Limitations

This study reported on the induction of macrophage M2 phenotype polarization by ADSC-Exos and the therapeutic effect of ADSC-Exos on T2DM lower extremity ischemia in mice. However, this study has certain limitations. First, this study only explored the role of the JAK/STAT6 signaling pathway in macrophage M2 polarization, but there are other signaling pathways that also mediated macrophage M2 polarization, which need to be explored. Second, previous studies indicate that there are a large number of beneficial miRNAs and proteins in exosomes. Our group has sequenced the miRNAs in ADSC-Exos and performed related functional experiments, which will be reported in future articles. Thirdly, it might be better if another control of exosomes from other non-ADSC cells such as fibroblast cells could be included in the experimental design. Finally, the mechanism through which M2 macrophages promote angiogenesis and revascularization in ischemic lower extremities is also a research hotspot. Further research is required to explore the specific mechanisms of the results reported in this study to create a suitable foundation for the clinical application of ADSC-Exos.

5. Conclusion

Our research indicated that ADSC-Exos can induce macrophage M2-phenotype polarization via the JAK/STAT6 signaling pathway, which enhances the viability, migration, and adhesion of macrophages, and promotes angiogenesis and blood perfusion in ischemic lower extremities of T2DM mice, providing novel insights for the clinical treatment of diabetic lower limb ischemic disease.

Declarations

Author contribution statement

Xiangkui Wang and Shiyuan Chen: Conceived and designed the experiments; Wrote the paper.

Ran Lu, Yong Sun, Tao Song and Zhonglin Nie: Performed the experiments; Analyzed and interpreted the data.

Chaowen Yu: Performed the experiments; Analyzed and interpreted the data; Wrote the paper.

Yong Gao: Conceived and designed the experiments.

Funding statement

Professor Yong Gao was supported by University Natural Science Research Project of Anhui Province [KJ2016SD38 & YJS20210538].

Data availability statement

Data will be made available on request.

Declaration of interests statement

The authors declare no conflict of interest.

Additional information

Supplementary content related to this article has been published online at https://doi.org/10.1016/j.heliyon.2022.e11495.

References

[1] J. Mills, M. Conte, D. Armstrong, F. Pomposelli, A. Schanzer, A. Sidawy, G. Andros, The society for vascular surgery lower extremity threatened limb classification system: risk stratification based on wound, ischemia, and foot infection (WIfI), J. Vasc. Surg. 59 (2014) 220–234, e221-222.

[2] Y. Shi, G. Hu, J. Su, W. Li, Q. Chen, P. Shou, C. Xu, X. Chen, Y. Huang, Z. Zhu, X. Huang, X. Han, N. Xie, G. Ren, Mesenchymal stem cells: a new strategy for immunosuppression and tissue repair, Cell Res 20 (2010) 510–518.

[3] A. Weiss, M. Dahlke, Immunomodulation by mesenchymal stem cells (MSCs): mechanisms of action of living, apoptotic, and dead MSCs, Front. Immunol. 10 (2019) 1191.

[4] X. Zhang, J. Qin, X. Wang, X. Guo, J. Liu, X. Wang, X. Wu, X. Lu, W. Li, X. Liu, Netrin-1 improves adipose-derived stem cell proliferation, migration, and treatment effect in type 2 diabetic mice with sciatic denervation, Stem Cell Res. Ther. 9 (2018) 285.

[5] M. Ratajczak, M. Kucia, T. Jadczyk, N. Greco, W. Wojakowski, M. Tendera, J. Ratajczak, Pivotal role of paracrine effects in stem cell therapies in regenerative medicine: can we translate stem cell-secreted paracrine factors and microvesicles into better therapeutic strategies? Leukemia 26 (2012) 1166–1173.

[6] R. Kalluri, V. LeBleu, The Biology Function and Biomedical Applications of Exosomes, Science, New York, N.Y., 2020, p. 367.

[7] X. Zhuang, X. Hu, S. Zhang, X. Li, X. Yuan, Y. Wu, Mesenchymal Stem Cell-Based Therapy as a New Approach for the Treatment of Systemic Sclerosis, Clinical reviews in allergy & immunology, 2022.

[8] E. Munoz-Perez, A. Gonzalez-Pujana, M. Igartua, E. Santos-Vizcaino, R. Hernandez, Mesenchymal stromal cell secretome for the treatment of immune-mediated inflammatory diseases: latest trends in isolation, content optimization and delivery avenues, Pharmaceutics 13 (2021).

[9] M. Piffoux, J. Volatron, K. Cherukula, K. Aubertin, C. Wilhelm, A. Silva, F. Gazeau, Engineering and loading therapeutic extracellular vesicles for clinical translation: a data reporting frame for comparability, Adv. Drug Deliv. Rev. 178 (2021), 113972.

[10] A. Psaraki, L. Ntari, C. Karakostas, D. Korrou-Karava, M. Roubelakis, Extracellular Vesicles Derived from Mesenchymal Stem/stromal Cells: the Regenerative Impact in Liver Diseases, Hepatology, Baltimore, Md, 2021.

[11] R. Yeo, R. Lai, B. Zhang, S. Tan, Y. Yin, B. Teh, S. Lim, Mesenchymal stem cell: an efficient mass producer of exosomes for drug delivery, Adv. Drug Deliv. Rev. 65 (2013) 336–341.

[12] A. Lapenna, M. De Palma, C. Lewis, Perivascular macrophages in health and disease, Nat. Rev. Immunol. 18 (2018) 689–702.

[13] P. Murray, Macrophage polarization, Annu. Rev. Physiol. 79 (2017) 541–566.

[14] S. Deng, X. Zhou, Z. Ge, Y. Song, H. Wang, X. Liu, D. Zhang, Exosomes from adipose-derived mesenchymal stem cells ameliorate cardiac damage after myocardial infarction by activating S1P/SK1/S1PR1 signaling and promoting macrophage M2 polarization, Int. J. Biochem. Cell Biol. 114 (2019), 105564.

[15] J. Li, H. Xue, T. Li, X. Chu, D. Xin, Y. Xiong, W. Qiu, X. Gao, M. Qian, J. Xu, Z. Wang, G. Li, Exosomes derived from mesenchymal stem cells attenuate the progression of atherosclerosis in ApoE mice via miR-let7 mediated infiltration and polarization of M2 macrophage, Biochem. Biophys. Res. Commun. 510 (2019) 565–572.

[16] D. Ti, H. Hao, C. Tong, J. Liu, L. Dong, J. Zheng, Y. Zhao, H. Liu, X. Fu, W. Han, LPS-preconditioned mesenchymal stromal cells modify macrophage polarization for resolution of chronic inflammation via exosome-shuttled let-7b, J. Transl. Med. 13 (2015) 308.

[17] P. Yang, J. Feng, Q. Peng, X. Liu, Z. Fan, Advanced glycation end products: potential mechanism and therapeutic target in cardiovascular complications under diabetes, Oxid. Med. Cell. Longev. 2019 (2019), 9570616.

[18] J. Groener, D. Oikonomou, R. Cheko, Z. Kender, J. Zemva, L. Kihm, M. Muckenthaler, V. Peters, T. Fleming, S. Kopf, P. Nawroth, Methylglyoxal and advanced glycation end products in patients with diabetes - what we know so far and the missing links, Exp. Clin. Endocrinol. Diabetes : official journal, German Society of Endocrinology [and] German Diabetes Association 127 (2019) 497–504.

[19] R. Lobb, M. Becker, S. Wen, C. Wong, A. Wiegmans, A. Leimgruber, A. Möller, Optimized exosome isolation protocol for cell culture supernatant and human plasma, J. Extracell. Vesicles 4 (2015), 27031.

[20] X. Zhang, Y. Jiang, Q. Huang, Z. Wu, H. Pu, Z. Xu, B. Li, X. Lu, X. Yang, J. Qin, Z. Peng, Exosomes derived from adipose-derived stem cells overexpressing glyoxalase-1 protect endothelial cells and enhance angiogenesis in type 2 diabetic mice with limb ischemia, Stem Cell Res. Ther. 12 (2021) 403.

[21] Y. Bi, J. Chen, F. Hu, J. Liu, M. Li, L. Zhao, M2 macrophages as a potential target for antiatherosclerosis treatment, Neural Plast 2019 (2019), 6724903.

[22] K. Zhang, X. Zhao, X. Chen, Y. Wei, W. Du, Y. Wang, L. Liu, W. Zhao, Z. Han, D. Kong, Q. Zhao, Z. Guo, Z. Han, N. Liu, F. Ma, Z. Li, Enhanced therapeutic effects of mesenchymal stem cell-derived exosomes with an injectable hydrogel for hindlimb ischemia treatment, ACS Appl. Mater. Interfaces 10 (2018) 30081–30091.

[23] P. Wu, B. Zhang, H. Shi, H. Qian, W. Xu, MSC-exosome: a novel cell-free therapy for cutaneous regeneration, Cytotherapy 20 (2018) 291–301.

[24] A. Casado-Díaz, J. Quesada-Gómez, G. Dorado, Extracellular vesicles derived from mesenchymal stem cells (MSC) in regenerative medicine: applications in skin wound healing, Front. Bioeng. Biotechnol. 8 (2020) 146.

[25] T. An, Y. Chen, Y. Tu, P. Lin, Mesenchymal stromal cell-derived extracellular vesicles in the treatment of diabetic foot ulcers: application and challenges, Stem Cell Rev. Rep. 17 (2021) 369–378.

[26] T. Polonsky, M. McDermott, Lower extremity peripheral artery disease without chronic limb-threatening ischemia: a review, JAMA 325 (2021) 2188–2198.

[27] A. Fakoya, New delivery systems of stem cells for vascular regeneration in ischemia, Front. Cardiovasc. Med. 4 (2017) 7.

[28] A. Mantovani, A. Sica, M. Locati, Macrophage polarization comes of age, Immunity 23 (2005) 344–346.

[29] J. Lambert, E. Lopez, M. Lindsey, Macrophage roles following myocardial infarction, Int. J. Cardiol. 130 (2008) 147–158.

[30] P. Manoonkitiwongsa, C. Jackson-Friedman, P. McMillan, R. Schultz, P. Lyden, Angiogenesis after stroke is correlated with increased numbers of macrophages: the clean-up hypothesis, J. Cerebr. Blood Flow Metabol. 21 (2001) 1223–1231.

[31] H. Liu, S. Antony, K. Roy, A. Juhasz, Y. Wu, J. Lu, J. Meitzler, G. Jiang, E. Polley, J. Doroshow, Interleukin-4 and interleukin-13 increase NADPH oxidase 1-related proliferation of human colon cancer cells, Oncotarget 8 (2017) 38113–38135.

[32] D. Zhou, C. Huang, Z. Lin, S. Zhan, L. Kong, C. Fang, J. Li, Macrophage polarization and function with emphasis on the evolving roles of coordinated regulation of cellular signaling pathways, Cell. Signal. 26 (2014) 192–197.

[33] S. Gordon, F. Martinez, Alternative activation of macrophages: mechanism and functions, Immunity 32 (2010) 593–604.

[34] Y. Chen, J. Zhang, S. Sun, [Comparison of three approaches to establishing Balb/c mouse models of hind-limb ischemia], Nan fang yi ke da xue xue bao, J. South. Med. Univ. 34 (2014) 1167–1170.

[35] M. McDermott, Lower extremity manifestations of peripheral artery disease: the pathophysiologic and functional implications of leg ischemia, Circ. Res. 116 (2015) 1540–1550.